

# High-efficiency Euclidean-based Models for Low-dimensional Knowledge Graph Embeddings

Kai Wang\*

School of Software, the Key  
Laboratory for Ubiquitous Network  
and Service Software of Liaoning  
Province, Dalian University of  
Technology  
Dalian, Liaoning, China  
kai\_wang@mail.dlut.edu.cn

Yu Liu

School of Software, the Key  
Laboratory for Ubiquitous Network  
and Service Software of Liaoning  
Province, Dalian University of  
Technology  
Dalian, Liaoning, China  
yuliu@dlut.edu.cn

Quan Z. Sheng

Intelligent Computing Laboratory  
Department of Computing  
Macquarie University  
Sydney, NSW, Australia  
michael.sheng@mq.edu.au

## ABSTRACT

Recent knowledge graph embedding (KGE) models based on hyperbolic geometry have shown great potential in a low-dimensional embedding space. However, the necessity of hyperbolic space in KGE is still questionable, because the calculation based on hyperbolic geometry is much more complicated than Euclidean operations. In this paper, based on the state-of-the-art hyperbolic-based model RotH, we develop two lightweight Euclidean-based models, called *RotL* and *Rot2L*. The RotL model simplifies the hyperbolic operations while keeping the flexible normalization effect. Utilizing a novel two-layer stacked transformation and based on RotL, the Rot2L model obtains an improved representation capability, yet costs fewer parameters and calculations than RotH. The experiments on link prediction show that Rot2L achieves the state-of-the-art performance on two widely-used datasets in low-dimensional knowledge graph embeddings. Furthermore, RotL achieves similar performance as RotH but only requires half of the training time. The source code of our work is available on GitHub.

## ACM Reference Format:

Kai Wang, Yu Liu, and Quan Z. Sheng. 2022. High-efficiency Euclidean-based Models for Low-dimensional Knowledge Graph Embeddings. In *Proceedings of ACM Conference (Conference'17)*. ACM, New York, NY, USA, 8 pages. <https://doi.org/10.1145/nnnnnnn.nnnnnnn>

## 1 INTRODUCTION

To represent entities and relations of knowledge graphs (KGs) in the semantic vector space, researchers have proposed various knowledge graph embedding (KGE) models, which have shown great potential in knowledge graph completion and knowledge-driven applications [7, 13, 19]. To achieve higher prediction accuracy, recent KGE models usually use high-dimensional embedding vectors up to 200 or even 500 dimensions [15, 21]. However, when

facing large-scale KGs with millions of entities, high embedding dimensions would require prohibitive training costs and storage space [12, 20]. It hinders the practical application of KGE models, especially in mobile smart devices.

Recently, low-dimensional KGE models based on hyperbolic vector space have drawn some attention [14]. The work of the first such model, MuRP, indicates that hyperbolic embeddings can capture hierarchical patterns in KGs and generate high-fidelity and parsimonious representations [1]. To capture logical patterns in KGs, Chami et al. propose a series of hyperbolic KGE models, including RotH, RefH, and AttH [8]. Similar to the typical TransE model [6] that treats the relation as a translation operation between the head and tail entity vectors, the state-of-the-art RotH model adjusts the head vector by the rotation and translation transformations to approach the tail vector in the hyperbolic space.

Although the above hyperbolic-based models outperform previous Euclidean-based models in low-dimensional condition, the necessity of hyperbolic space in this task is still questionable. Comparing a hyperbolic model with its Euclidean-based variant, it is uncertain what part of the modification is vital. Besides, despite theoretical support, the Möbius matrix-vector multiplication and Möbius addition operations in hyperbolic embeddings are far more complicated than Euclidean multiplication and addition. As shown in Fig. 1, RotH requires threefold more training time than its Euclidean-based variant RotE on two datasets. When processing large-scale knowledge graphs, the additional calculating cost caused by the complicated hyperbolic operations would make the problem much severer.

Facing these problems, we analyze the effective components in the hyperbolic KGE models, and propose two lightweight “RotH-like” models, RotL and Rot2L, for low-dimensional knowledge graph embeddings. Without the hyperbolic geometry, RotL eliminates the Möbius matrix-vector multiplication and designs a new flexible addition operation to replace the Möbius addition. To further improve the RotL’s representation capability, the Rot2L model utilizes two stacked rotation-translation transformations in the Euclidean space. Benefiting from a specific parameterization strategy, Rot2L requires fewer parameters and calculations than RotH.

We conduct extensive experiments on two widely-used datasets, FB15k-237 [16] and WN18RR [5]. The results show that RotL outperforms existing Euclidean-based models in the 32-dimensional condition and only requires half of the training time of RotH. Rot2L

\*Corresponding author

Permission to make digital or hard copies of all or part of this work for personal or classroom use is granted without fee provided that copies are not made or distributed for profit or commercial advantage and that copies bear this notice and the full citation on the first page. Copyrights for components of this work owned by others than ACM must be honored. Abstracting with credit is permitted. To copy otherwise, or republish, to post on servers or to redistribute to lists, requires prior specific permission and/or a fee. Request permissions from [permissions@acm.org](mailto:permissions@acm.org).

Conference’17, July 2017, Washington, DC, USA

© 2022 Association for Computing Machinery.

ACM ISBN 978-x-xxxx-xxxx-x/YY/MM.

<https://doi.org/10.1145/nnnnnnn.nnnnnnn>

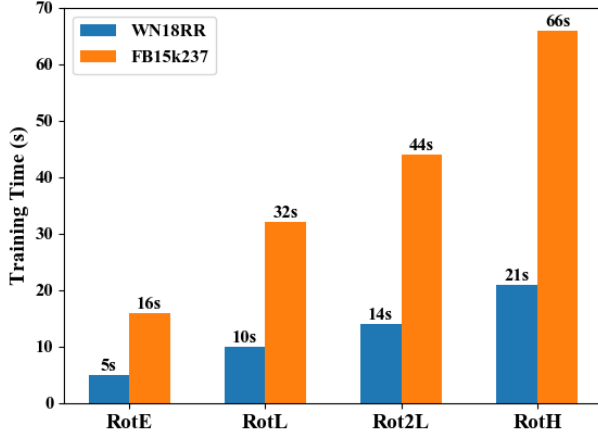


**Figure 1: The training time per epoch of different 32-dimensional models on two datasets. All results are measured under the same parameter settings (500 batch size and 500 negative samples). RotL and Rot2L are the models proposed in this paper.**

obtains the state-of-the-art performance on the two datasets and outperforms RotH in both prediction accuracy and training speed. According to ablation experiments, we prove the effectiveness of the flexible addition and the other significant modules in Rot2L. We also verify our models in different embedding dimensions and analyze the performance difference between RotH and our models in a relation-specific experiment.

## 2 BACKGROUND AND RELATED WORK

In this section, we briefly describe the preliminaries and related work on KGE.

### 2.1 Knowledge Graph Embeddings

In a knowledge graph  $\mathcal{G} = (E, R, T)$ ,  $E$  and  $R$  denote the set of entities and relations, and  $T$  is the collection of factual triples  $(h, r, t)$  where the head and tail entities  $h, t \in E$  and the relation  $r \in R$ .  $N_e$  and  $N_r$  refer to the number of entities and relations, respectively.

Knowledge graph embeddings aim to represent each entity  $e$  and each relation  $r$  as  $d$ -dimensional continuous vectors. A KGE model is evaluated by the link prediction task, which aims to find  $e_t \in E$  given an e-r query  $q = (e, r)$ , such that the triple  $(e, r, e_t)$  or  $(e_t, r, e)$  should belong to the knowledge graph  $\mathcal{G}$ . Generally, a scoring function  $F(h, r, t) = D(Q(h, r), t)$  is designed to measure each candidate triple, which involves two operations: 1) *Transformation function*  $Q(h, r)$  transforms the head vector  $\mathbf{h}$  using the relation vector  $\mathbf{r}$ ; 2) *Distance function*  $D(q, t)$  measures the distance between the tail vector  $\mathbf{t}$  and the transformed head vector  $\mathbf{q}$ .

Various KGE models have been proposed using different scoring functions, such as translation-based TransE [6], factorization-based ComplEx [17] and CNN-based ConvE [9]. Recently, Balazevic et al. [2] proposed a linear model based on Tucker decomposition of the binary tensor representation of knowledge graph triples. RotatE [15], inspired by Euler’s identity, represents a relation as the rotation operation between the head and tail entities.

### 2.2 Hyperbolic Geometry

Multiple hyperbolic KGE models proposed very recently have achieved good performance in low-dimensional condition, such as MuRP, RotH, RefH and AttH [1, 8]. These models employ a hyperbolic geometry model, the  $d$ -dimensional Poincaré ball [4] with negative curvature  $-c$  ( $c > 0$ ):  $\mathbb{B}_c^d = \{x \in \mathbb{R}^d : \|x\|^2 < \frac{1}{c}\}$ , where  $\|\cdot\|$  denotes the  $L_2$  norm.

To achieve the vector transformation in the hyperbolic space, the Möbius addition  $\oplus_c$  and Möbius matrix-vector multiplication  $\otimes_c$  are utilized. Möbius addition [18] is proposed to approximate Euclidean addition in the hyperbolic space:

$$x \oplus_c y = \frac{(1 + 2c\langle x, y \rangle + c\|y\|^2)x + (1 - c\|x\|^2)y}{1 + 2c\langle x, y \rangle + c^2\|x\|^2\|y\|^2} \quad (1)$$

where  $\langle \cdot \rangle$  is the Euclidean inner product. It is clear that Möbius addition requires much more calculations than an ordinary addition.

Möbius matrix-vector multiplication [10] is also more complicated than Euclidean multiplication. Before computing matrix multiplication with  $M \in \mathbb{R}^{d \times k}$ , the vector  $x \in \mathbb{B}_c^d$  is projected onto the tangent space at  $0 \in \mathbb{B}_c^d$  with the *logarithmic map*  $\log_0^c(x)$ . Then the output of multiplication is projected back to  $\mathbb{B}_c^d$  via the *exponential map*  $\exp_0^c(x)$ , i.e.,

$$M \otimes_c x = \exp_0^c(M \log_0^c(x)) \quad (2)$$

$$\exp_0^c(x) = \tanh(\sqrt{c}\|x\|) \frac{x}{\sqrt{c}\|x\|} \quad (3)$$

$$\log_0^c(x) = \operatorname{arctanh}(\sqrt{c}\|x\|) \frac{x}{\sqrt{c}\|x\|} \quad (4)$$

### 2.3 The RotH Model

We briefly review RotH [8], the state-of-the-art model in the low-dimensional KGE. The scoring function of RotH employs a “translation-rotation-translation” transformation and utilizes a hyperbolic distance as the distance function  $D$ .

Specifically, let  $\mathbf{e}^H \in \mathbb{B}_c^d$  denote entity hyperbolic embeddings of entity  $e$ . For one relation  $r$ , two hyperbolic relation vectors  $\mathbf{r}^H, \mathbf{r}'^H \in \mathbb{B}_c^d$  are defined for two translation operations. Using a  $d$ -dimensional vector  $\hat{\mathbf{r}}$ , RotH parameterizes a *Givens Rotation* operation with a block-diagonal matrix of the form:

$$\operatorname{Rot}(\hat{\mathbf{r}}) = \operatorname{diag}(G(\hat{r}_1, \hat{r}_2), \dots, G(\hat{r}_{d-1}, \hat{r}_d)) \quad (5)$$

$$\text{where } G(\hat{r}_i, \hat{r}_j) := \begin{bmatrix} \hat{r}_i & -\hat{r}_j \\ \hat{r}_j & \hat{r}_i \end{bmatrix}. \quad (6)$$

Then, for a triple  $(h, r, t)$ , the scoring function  $F_H$  of RotH is defined as:

$$Q_H^c(h, r) = \operatorname{Rot}(\hat{\mathbf{r}}) \otimes_c (\mathbf{h}^H \oplus_c \mathbf{r}^H) \oplus_c \mathbf{r}'^H \quad (7)$$

$$D_H^c(q, t) = -\frac{2}{\sqrt{c}} \operatorname{arctanh}(\sqrt{c}\|q - q \oplus_c t^H\|) \quad (8)$$

$$F_H(h, r, t) = D_H^{c_r}(Q_H^{c_r}(h, r), t) + b_h + b_t, \quad (9)$$

where  $c_r > 0$  is the relation-specific curvature parameter, and  $b_e (e \in E)$  are entity biases which act as margins in the scoring function [1, 8].

The other hyperbolic models can be regarded as RotH’s variants using different relation transformations. In addition, RotE is an

Euclidean-based RotH variant, and its scoring function is defined as:

$$F_E(h, r, t) = -\|(Rot(\hat{r})h + r) - t\|^2 + b_h + b_t, \quad (10)$$

where  $h, r, t \in \mathbb{R}^d$ . Without complex hyperbolic calculations,  $F_E$  can be computed in linear time of the embedding dimensions.

### 3 THE METHODOLOGY

The goal of this work is to design a high-efficiency low-dimensional KGE model by extracting the effective components in the RotH model and eliminating the redundancy. In our preliminary experiments, we find that RotH performs noticeably well because of two reasons. The first reason is *rotation-translation transformation*. As proved in previous research [8, 15], this specific transforming operation can infer different relation patterns in the KG. Benefiting from the rotation-translation transformation, both RotH and its Euclidean-based variant RotE achieve great prediction accuracy in high-dimensional KGE. The second reason is *flexible normalization*. All entity vectors in the hyperbolic space satisfy  $\|e\|^2 < \frac{1}{c}$  before and after transformation, while the curvature  $c$  is relation-specific and self-adaptive. As the representation capability of a low-dimensional vector space is limited, the effect of flexible normalization would be more obvious. It explains why RotH can outperform RotE in low-dimensional KGE tasks.

In this section, we first propose a lightweight model, called RotL, which remains the flexible normalization of RotH and simplifies the complex hyperbolic operations. The details of RotL will be described in Sec. 3.1. We further design the Rot2L model using two stacked rotation-translation transformations. Rot2L employs a novel parameterization strategy that can save half of parameters in the two-layer architecture. We will detail Rot2L in Sec. 3.2, followed by an efficiency analysis in Sec 3.3. The architectures of the four models mentioned above are illustrated in Fig. 2.

#### 3.1 The RotL Model and Flexible Addition

The RotL model aims to achieve similar performance to RotH and minimize its computational complexity close to that of RotE. Comparing the scoring functions of RotH and RotE in Eq. 9 and 10, it is clear that the additional calculations of RotH are centered on Möbius addition and Möbius matrix-vector multiplication.

Therefore, we first eliminate the hyperbolic embeddings in RotL and initialize the entity vector  $e$  and the two relation vectors for rotation and translation in the Euclidean space, such that the relation transformation can be calculated using Euclidean addition and multiplication directly.

To achieve the flexible normalization, we propose Flexible Addition  $\oplus_\alpha$ , a simplified form of Möbius Addition, i.e.,

$$x \oplus_\alpha y = \frac{\alpha(x + y)}{1 + \langle x, y \rangle}, \quad (11)$$

where  $\alpha$  is a relation-specific scaling parameter and with a default value of 1. The Flexible Addition provides a self-adaptive normalization to  $(x + y)$ , and has lower computational complexity than Möbius addition. Counting the operation times of  $d$ -dimensional vector operations, the former requires three additions and two multiplications, while the latter needs nine and 12 operations,

respectively. We further discuss the connection between the two operations through Theorem 1.

**Theorem 1.** Given that  $c = \alpha = 1$ , the Möbius Addition is equivalent to Flexible Addition, i.e.,  $x \oplus_c x \equiv x \oplus_\alpha x$ .

*Proof.* With  $c = \alpha = 1$ ,

$$\begin{aligned} x \oplus_c y &= \frac{(1 + 2\langle x, y \rangle + \|y\|^2)x + (1 - \|x\|^2)y}{1 + 2\langle x, y \rangle + \|x\|^2\|y\|^2} \\ &= \frac{(1 + \langle x, y \rangle + \langle y, x \rangle + \|y\|^2)x + (1 - \|x\|^2)y}{1 + \langle x, y \rangle + \langle y, x \rangle + \|x\|^2\|y\|^2} \\ &= \frac{(1 + \langle y, x \rangle)(x + y)}{(1 + \langle x, y \rangle)(1 + \langle y, x \rangle)} = \frac{x + y}{1 + \langle x, y \rangle} = x \oplus_\alpha y \end{aligned} \quad (12)$$

We then define the transformation function of RotL as  $Q_L^\alpha(h, r) = Rot(\hat{r})h \oplus_\alpha r'$ , which can be regarded as a RotE transformation using the flexible addition. To fit this novel operation, we further modify the distance function of RotH in Eq. 8 by designing a simpler non-linear mapping operation. The distance function and scoring function of RotL are defined as follows:

$$D_L^\alpha(q, t) = -\varphi(\| -q \oplus_\alpha t \|) \quad (13)$$

$$F_L(h, r, t) = D_L^{\alpha_r'}(Q_L^{\alpha_r}(h, r), t) + b_h + b_t, \quad (14)$$

where  $\varphi(x) = xe^x$ ,  $\alpha_r$  and  $\alpha_r'$  are two different scaling parameters.

Comparing Eq. 9 and ??, it is clear that the hyperbolic calculations are completely eliminated in the RotL model. Thus, RotL can reduce the computation complexity of RotH and save half of the training time as shown in Fig. 1.

#### 3.2 The Rot2L Model and Stacked Transformation

Although the lightweight RotL maintains the flexible normalization effect, its performance is limited by the original transformation function of RotH. In this section, we describe a novel Rot2L model utilizing two stacked translation-rotation transformations.

According to the theory of affine transformation [3], the two transformations can be replaced by a single one. Therefore, inspired by neural networks, we design a two-layer architecture with an activate function in the middle, as shown in Fig. 2. The transformation function  $Q_{2L}(h, r, t)$  in Rot2L is defined as:

$$\varrho(h, q) = \tanh(q) + \gamma h \quad (15)$$

$$Q_{2L}^{\alpha^1, \alpha^2}(h, r) = Q_L^{\alpha^1}(\varrho(h, Q_L^{\alpha^2}(h, r)), r), \quad (16)$$

where  $\gamma$  is a hyper-parameter that balances the two parts.  $Q_L^{\alpha^1}$  and  $Q_L^{\alpha^2}$  represent two transformation layers, which are same with the transformation function in RotL.

In the Rot2L model, the two layers need different parameters. This would double the amount of relation parameters because each layer requires two  $N_r \times d$  embedding matrices to represent the translation vectors and rotation matrices for all relations. To reduce relation parameters, Rot2L employs a novel parameterization strategy, which shares partial parameters among different relations.

Specifically, we utilize one embedding matrix  $M \in \mathbb{R}^{N_r \times d}$  and a  $d$ -dimensional learnable vector  $f \in \mathbb{R}^d$  for each rotation-translation transformation layer. Such that half of the parameters are shared in different relations by replacing another embedding

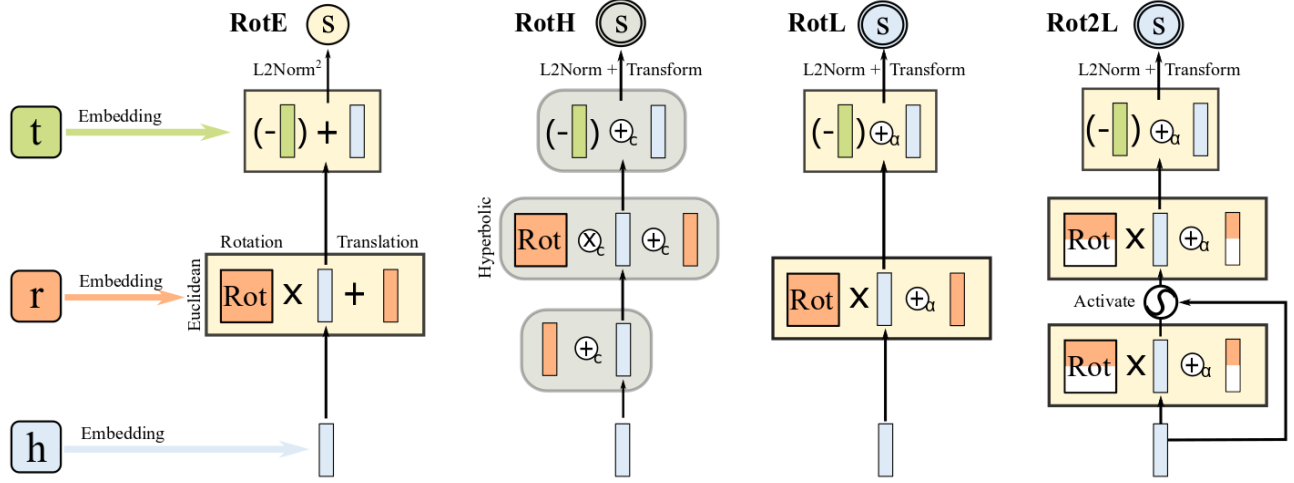


**Figure 2: The architectures of four models, including the previous RotE and RotH, and the proposed RotL and Rot2L in this paper. The rectangle box denotes an Euclidean-based operation, while the rounded rectangle box denotes a hyperbolic-based one. The inside rectangles denotes the embedding vectors or matrices, in which the relation-specific ones are in orange.  $\otimes_c$ ,  $\oplus_c$ ,  $\oplus_\alpha$  refer to Möbius multiplication, Möbius addition and Flexible addition, respectively.**

matrix to the vector  $f$ . Given the vector  $r = M[r]$  for the relation  $r$ , the corresponding translation vector and rotation matrix are constructed as:

$$r' = [r_1, f_1, r_2, f_2, \dots, r_{\frac{d}{2}}, f_{\frac{d}{2}}], \quad (17)$$

$$Rot(\hat{r}) = \text{diag}(G(r_{\frac{d}{2}+1}, f_{\frac{d}{2}+1}), \dots, G(r_d, f_d)), \quad (18)$$

Finally, the scoring function of Rot2L contains the transformation function  $Q_{2L}(h, r, t)$  and the same distance function as RotL, which is defined as:

$$F_L(h, r, t) = D_L^{\alpha_r}(Q_{2L}^{\alpha_1 r, \alpha_2 r}(h, r), t) + b_h + b_t. \quad (19)$$

Note that, it might be feasible to employ more transformation layers in Rot2L like deep neural networks. There are two reasons that we do not utilize more than two layers. First, more layers require more parameters, which goes against our original intention of being lightweight. Second, we find the vector values are gradually magnified when getting through multiple layers. Using three layers in the Rot2L model already suffers performance decrease. Exploring a deeper model with more effective regularization will be our future work.

### 3.3 Efficiency Analysis

We analyze and compare the computational complexity among RotE, RotH, RotL, and Rot2L in this section. In terms of time complexity, as shown in Fig. 1, RotL is much faster than RotH mainly because that the Flexible Addition requires only a quarter of the computational cost of the Möbius addition. Although Rot2L repeats the rotation-translation transformation twice, its computational cost is still lower than that of RotH.

In terms of space complexity, a slight difference is shown in the number of relation parameters. Because the parameters related to entities, including entity embedding vectors and entity biases,

are the same in the four models and occupy the vast majority of total parameters. RotH requires the most relation parameters,  $(3N_r + 1)d$ , including three relation transformation vectors and the learnable curvature for different relations. By contrast, RotE and RotL cost smaller, which are  $2N_r d$  and  $2(N_r + 1)d$ , and the extra part of RotL comes from  $\alpha$  in Flexible Addition. Although using an effective parameterization strategy, Rot2L still requires two shared vectors and another  $\alpha$ -related vector. Its relation parameter amount is  $(2N_r + 5)d$ . As the relation number  $N_r$  is always greater than four, the Rot2L model still requires fewer parameters than RotH.

In summary, the RotL and Rot2L models are highly efficient and better than the RotH model in both time complexity and space complexity.

## 4 EXPERIMENTS

### 4.1 Experimental Setup

**Datasets.** Our experimental studies are conducted on two widely-used datasets. WN18RR [5] is a subset of the English lexical database WordNet [11], while FB15k237 [16] is extracted from Freebase including knowledge facts on movies, actors, awards, and sports. Inverse relations are removed from the two datasets, as many test triples can be obtained simply by inverting triples in the training set. The statistics of the datasets are given in Table 1 and “Train”, “Valid”, “Test” refer to the amount of triples in training, validation, and test sets.

**Table 1: Statistics of the datasets.**

Dataset	$N_r$	$N_e$	#Train	#Valid	#Test
FB15k237	237	14,541	272,115	17,535	20,466
WN18RR	11	40,943	86,845	3,034	3,134

**Table 2: The link prediction results on the FB15k237 and WN18RR datasets. The best scores of 32-dimensional models are in Bold.**

Type	Methods	FB15K237			WN18RR		
		MRR	Hits@10	Hits@1	MRR	Hits@10	Hits@1
Euclidean-based Models	RotatE	0.290	0.458	0.208	0.387	0.491	0.330
	TuckER	0.306	0.475	0.223	0.428	0.474	0.401
	MuRE	0.313	0.489	0.226	0.458	0.525	0.421
	RefE	0.302	0.474	0.216	0.455	0.521	0.419
	RotE	0.307	0.482	0.220	0.463	0.529	0.426
	AttE	0.311	0.488	0.223	0.456	0.526	0.419
Hyperbolic-based Models	MuRP	0.317	0.497	0.229	0.464	0.544	0.424
	RefH	0.312	0.489	0.224	0.447	0.518	0.408
	RotH	0.314	0.497	0.223	0.472	0.553	0.428
	AttH	0.316	0.495	0.227	0.464	0.551	0.424
Our Models	<b>RotL</b>	0.316	0.496	0.228	0.469	0.550	0.426
	<b>Rot2L</b>	<b>0.321</b>	<b>0.502</b>	<b>0.231</b>	<b>0.475</b>	<b>0.554</b>	<b>0.434</b>

**Implementation Details.** Following the previous work [15], we utilize a negative sampling loss, which is defined as:

$$L = -\log\sigma(F(h, r, t)) - \sum_{i=0}^k p_i \log\sigma(-F(h'_i, r, t'_i)), \quad (20)$$

where  $\sigma(\cdot)$  refers to the Sigmoid function,  $\{h'_i, r, t'_i\}$  are the negative samples, and their weights  $\{p_i\} = \text{Softmax}(\{F(h'_i, r, t'_i)\})$ . All experiments are performed on Intel Core i7-7700K CPU @ 4.20GHz and NVIDIA GeForce GTX1080 Ti GPU, and implemented in Python using the PyTorch framework.

**Hyperparameter Settings.** According to the low dimensional condition, we train our model with the Adam optimizer setting the embedding dimensions in  $\{8, 16, 32, 64\}$ . We select the hyper-parameters of our model via grid search according to the metrics on the validation set. Specifically, we empirically select the learning rate among  $\{0.0005, 0.001, 0.005\}$ , the batch size among  $\{100, 200, 500\}$ , the amount of negative samples  $k$  among  $\{50, 200, 500\}$ , and the balance hyper-parameter  $\gamma$  among  $\{0.1, 0.3, 0.5, 1.0\}$ .

**Evaluation Metrics.** For the link prediction experiments, we adopt three evaluation metrics: 1) MRR, the average inverse rank of the test triples, 2) Hits@10, the proportion of correct entities ranked in top 10, and 3) Hits@1, the proportion of correct entities ranked first. Higher MRR, Hits@10, and Hits@1 mean better performance. Following the previous works, we process the output sequence in the filter mode.

## 4.2 Link Prediction Task

We evaluate our models in the link prediction task on the two datasets. The experimental results are shown in Table 2. We select ten compared models in two types, in which the first 6 models are Euclidean-based, and the others utilize hyperbolic embeddings. All of these models are in 32-dimensional vector space, which is the same as the low-dimensional setting of Chami et al. [8].

From the results, we have the following observations. At first, the four hyperbolic-based models generally outperform their Euclidean variants and RotatE and TuckER, which are the state-of-the-art models for high-dimensional knowledge graph embeddings. This

proves the effectiveness of hyperbolic models in low-dimensional knowledge graph embeddings.

RotL outperforms RotE and the other Euclidean-based models. Compared with RotE, the Hits@10 of RotL improves from 0.529 to 0.550 on WN18RR, and from 0.482 to 0.496 on FB15k237. RotL achieves similar prediction accuracy as RotH. Using a lightweight architecture, RotL even obtains higher MRR and Hits@1 than RotH on FB15k237. It indicates that the hyperbolic embeddings technology is possible to be replaced with flexible addition and new distance function.

Using a novel two-layer transformation function, Rot2L further improves RotL and achieves the state-of-the-art results on the both datasets. Especially compared with RotH, MRR of Rot2L improves from 0.314 to 0.321 on FB15k237, and the Hits@1 increases from 0.428 to 0.434 on WN18RR. Although the published results of AttH is competitive [8], we cannot reproduce them using the available open-source codes. Besides, AttH costs more calculations than RotH, and much slower than our proposed Rot2L.

It should be noted that improving low-dimensional performance is much harder than that in the high-dimensional condition. The computational complexity of Rot2L is lower than RotH and AttH, and our experimental results prove the effectiveness of Rot2L.

## 4.3 Ablation Studies

We further conduct a series of ablation experiments to evaluate the different modules of our models. Two main improvements should be evaluated: 1) the new distance function (Dis) in Eq. 13 and 2) the middle activate function (Mid) in Eq. 15. Accordingly, we test the variants by eliminating one of the two functions (e.g., Rot2Lw/oMid by removing the distance function). The other parts, such as flexible addition and stacked transformations, can be verified by comparing RotE (an Euclidean-based variant of RotH), RotL and Rot2L. The experimental results are shown in Table 3.

From the results, we can see that Hits@10 of Rot2L are higher than Rot2Lw/oDis on the both datasets, which proves the effectiveness of the distance function. Similar result is also shown in RotL, but the improvement is relatively small. Hits@10 of Rot2Lw/oMid are lower than that of Rot2L on FB15k237, while having no obvious difference on WN18RR. This indicates

**Table 3: The results of ablation experiments on (a) FB15k237 and (b) WN18RR.**

Methods	FB15K237		
	MRR	Hits@10	Hits@1
Rot2L	<b>0.321</b>	<b>0.502</b>	<b>0.231</b>
Rot2Lw/oMid	0.315	0.494	0.227
Rot2Lw/oDis	0.314	0.490	0.225
RotL	0.316	0.496	0.228
RotLw/oDis	0.315	0.492	0.227
RotE	0.307	0.482	0.220

(a)

Methods	WN18RR		
	MRR	Hits@10	Hits@1
Rot2L	<b>0.476</b>	<b>0.554</b>	<b>0.436</b>
Rot2Lw/oMid	0.474	0.554	0.435
Rot2Lw/oDis	0.463	0.543	0.426
RotL	0.469	0.550	0.426
RotLw/oDis	0.467	0.549	0.420
RotE	0.463	0.529	0.426

(b)

that the activate function is more effective on FB15k237, which contains much more relations than WN18RR. For FB15k237, RotL outperforms Rot2Lw/oMid, indicating that facing complex relationships, the pure two-layer transformation is no better than a single layer. This further validates the contribution of the activate function. Comparing RotLw/oDis and RotE, the impact of flexible addition is obvious. Using a simple scaling operation, the flexible addition provides a 1% and 2% improvements of Hits@10 on the two datasets, respectively.

Overall, the experimental results indicate the effectiveness of the major modules of our proposed models in this paper. Based on the same Euclidean space, our RotL and Rot2L models have a significant performance improvement compared to the RotE model.

## 5 DISCUSSION

In this section, we further discuss several important questions on the RotL and Rot2L models.

### Q1: Which parts of predictions are improved in our models comparing with RotH?

We measure the prediction performance of relation-specific triples on WN18RR in Table 4 to analyze the improvements of the Rot2L model. Comparing in different relations, RotE and RotH have their own strengths. RotH has better Hits@10 in most relations but is weaker than RotE in the “member of domain usage” and “member of domain region” relations. RotL performs well like RotH, but fails to predict the “similar to” relation. As the optimal model, Rot2L obtains the best Hits@10 in 8 out of 11 relations and only has a small decrease in the other three relations. It should be noted that RotL and Rot2L effectively improve on the two “member of” relations, comparing to RotH. Especially, Rot2L achieves 42.86% and 64.27% improvements than RotH on these relations. Achieving the flexible normalization of RotH in the Euclidean space, our models perform well in both RotH-dominant and RotE-dominant relations.

### Q2: How about the model performance in other embedding dimensions?

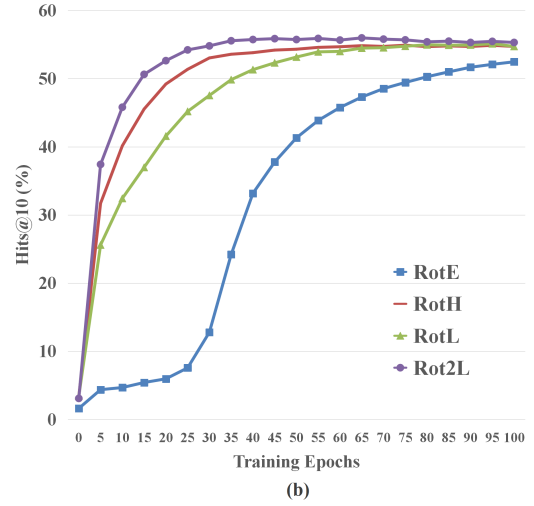
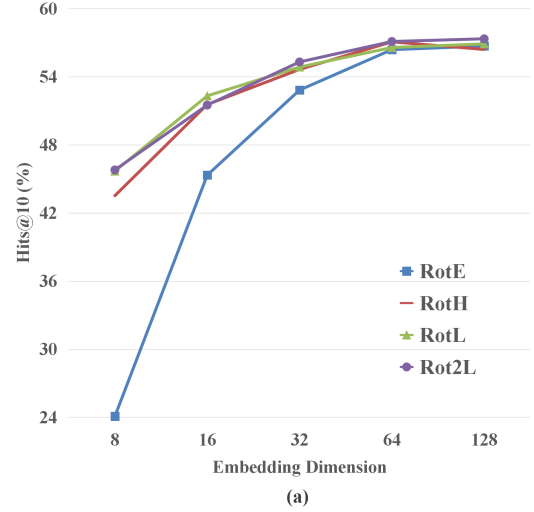


**Figure 3: (a) The Hits@10 of four models on WN18RR with different embedding dimensions. (b) The changes of the Hits@10 on WN18RR as training proceeds.**

We further compare the four models in different dimensions from 8 to 128. The experimental results are shown in Fig. 3(a). The prediction accuracy of the four models improves with the growth of the embedding dimensions. When the dimensions are lower than 32, RotE is obviously weaker than the others, but it performs well in the high-dimensional condition. This result indicates the necessity to research the low-dimensional KGE models. Except for RotE, the other three models obtain similar results under different dimensions, but there are still some differences. Specifically, RotL performs better in lower dimensions and achieves the best Hits@10 under 16 dimensions. The advantage of Rot2L is shown with the increase of dimensions: Rot2L outperforms the other two after 32 dimensions. It proves that the stacked transformations in Rot2L have stronger representation capacity in the high-dimensional condition.

### Q3: Can our models accelerate the training speed?



**Table 4: Comparison of Hits@10 on relation-specific triples in WN18RR.  $\Delta(\text{L-H})$  denotes the growth rate of RotL relative to RotH, and similarly  $\Delta(2\text{L-H})$  denotes the growth rate of Rot2L.**

Relation	RotE	RotH	RotL	$\Delta(\text{L-H})$	Rot2L	$\Delta(2\text{L-H})$
hypernym	0.242	0.250	0.247	-1.12%	<b>0.254</b>	1.44%
derivationally related form	0.960	<b>0.970</b>	0.967	-0.24%	0.968	-0.15%
instance hypernym	<b>0.533</b>	0.480	0.496	3.42%	0.467	-2.57%
verb group	<b>0.974</b>	<b>0.974</b>	<b>0.974</b>	0.00%	<b>0.974</b>	0.00%
also see	0.634	0.643	0.625	-2.78%	<b>0.688</b>	6.95%
has part	0.343	<b>0.349</b>	0.329	-5.83%	0.334	-4.17%
<b>member of domain usage</b>	0.375	0.292	<b>0.417</b>	42.86%	<b>0.417</b>	42.86%
<b>member of domain region</b>	0.365	0.269	0.385	42.86%	<b>0.442</b>	64.27%
similar to	<b>1.000</b>	<b>1.000</b>	0.667	-33.34%	<b>1.000</b>	0.00%
member meronym	0.342	0.395	0.405	2.49%	<b>0.451</b>	14.00%
synset domain topic of	0.382	0.408	0.439	7.53%	<b>0.443</b>	8.61%

Fig. 3 (b) shows the convergence of the training process for the four models under 32 dimensions. We can observe that RotE increases slowly in the first 20 epochs and converges much later than the others. RotH converges faster than RotE, which is previously regarded as the contribution of hyperbolic space.

From our experimental results, it is clear that both RotL and Rot2L show similar performance. RotL, which has little difference from RotE in structure, shows a much faster training speed. Although rote learning takes less time over one epoch, RotL can complete the training process in a much shorter time. Comparing RotH and Rot2L, we can find that Rot2L precedes in almost every epoch. In the 25th epoch, Rot2L already achieves similar performance to the final performance of RotH.

The results indicate that our models can replace the hyperbolic RotH model with comparable prediction accuracy and training speed.

## 6 CONCLUSION

The recently proposed hyperbolic-based models achieve great prediction accuracy in low-dimensional knowledge graph embeddings, but require complicated calculations for hyperbolic embeddings. It would cause unbearable computational costs when processing large-scaled knowledge graphs. In this paper, we analyze the effective components in those models and propose a lightweight variant based on Euclidean calculations. After simplifying the Möbius operations in RotH, our proposed RotL model achieves a competitive performance, which saves half of the training time. Using a two-layer stacked transformation, we further propose Rot2L that outperforms the state-of-the-art RotH model in both prediction accuracy and training speed.

These positive results encourage us to explore further research activities in the future. We will theoretically analyze the effectiveness of flexible normalization in the low-dimensional KGE tasks. For the stacked transformations in Rot2L, we will explore multiple-layer architectures and evaluate more different transformation forms. Finally, we plan to apply our models on real-world knowledge graphs in different domains such as mobile healthcare, smart cities, and mobile e-Commerce.

## REFERENCES

- [1] Ivana Balazević, Carl Allen, and Timothy M. Hospedales. 2019. Multi-relational Poincaré Graph Embeddings. In *Advances in Neural Information Processing Systems 32: Annual Conference on Neural Information Processing Systems 2019, NeurIPS 2019, 8-14 December 2019, Vancouver, BC, Canada*. 4465–4475.
- [2] Ivana Balazević, Carl Allen, and Timothy M. Hospedales. 2019. TuckER: Tensor Factorization for Knowledge Graph Completion. In *Proceedings of the 2019 Conference on Empirical Methods in Natural Language Processing, EMNLP-IJCNLP, 2019*. 5184–5193.
- [3] Marcel Berger. 1987. *Geometry I*. Springer Berlin Heidelberg.
- [4] G. Birman and A. Ungar. 2001. The hyperbolic derivative in the Poincaré ball model of hyperbolic geometry. *J. Math. Anal. Appl.* 254 (2001), 321–333.
- [5] Antoine Bordes, Xavier Glorot, Jason Weston, and Yoshua Bengio. 2014. A semantic matching energy function for learning with multi-relational data. *Machine Learning* 94 (2014), 233–259.
- [6] Antoine Bordes, Nicolas Usunier, Alberto García-Durán, Jason Weston, and Oksana Yakhnenko. 2013. Translating Embeddings for Modeling Multi-relational Data. In *Proceedings of Advances in Neural Information Processing Systems (NIPS 2013)*. 2787–2795.
- [7] Samuel Broscheit, Kiril Gashteovski, Yanjie Wang, and Rainer Gemulla. 2020. Can We Predict New Facts with Open Knowledge Graph Embeddings? A Benchmark for Open Link Prediction. In *Proceedings of the 58th Annual Meeting of the Association for Computational Linguistics, ACL 2020, Online, July 5-10, 2020*. 2296–2308.
- [8] Ines Chami, Adva Wolf, Da-Cheng Juan, Frederic Sala, Sujith Ravi, and Christopher Ré. 2020. Low-Dimensional Hyperbolic Knowledge Graph Embeddings. In *Proceedings of the 58th Annual Meeting of the Association for Computational Linguistics, ACL 2020, Online, July 5-10, 2020*. 6901–6914.
- [9] Tim Dettmers, Pasquale Minervini, Pontus Stenetorp, and Sebastian Riedel. 2018. Convolutional 2D Knowledge Graph Embeddings. In *Proceedings of the 32th AAAI Conference on Artificial Intelligence*. 1811–1818.
- [10] Octavian-Eugen Ganea, Gary Bécigneul, and Thomas Hofmann. 2018. Hyperbolic Neural Networks. In *Advances in Neural Information Processing Systems 31: Annual Conference on Neural Information Processing Systems 2018, NeurIPS 2018, 3-8 December 2018, Montréal, Canada*. 5350–5360.
- [11] George A. Miller. 1995. WORDNET: A Lexical Database for English. *Commun. ACM* 38 (1995), 39–41.
- [12] Mrinmaya Sachan. 2020. Knowledge Graph Embedding Compression. In *Proceedings of the 58th Annual Meeting of the Association for Computational Linguistics, ACL 2020, Online, July 5-10, 2020*. 2681–2691.
- [13] Apoorv Saxena, Aditya Tripathi, and Partha P. Talukdar. 2020. Improving Multi-hop Question Answering over Knowledge Graphs using Knowledge Base Embeddings. In *Proceedings of the 58th Annual Meeting of the Association for Computational Linguistics, ACL 2020, Online, July 5-10, 2020*. 4498–4507.
- [14] Zequn Sun, Muhao Chen, Wei Hu, Chengming Wang, Jian Dai, and Wei Zhang. 2020. Knowledge Association with Hyperbolic Knowledge Graph Embeddings. In *Proceedings of the 2020 Conference on Empirical Methods in Natural Language Processing, EMNLP 2020, Online, November 16-20, 2020*. 5704–5716.
- [15] Zhiqing Sun, Zhihong Deng, Jianyun Nie, and Jian Tang. 2019. RotatE: Knowledge Graph Embedding by Relational Rotation in Complex Space. In *7th International Conference on Learning Representations, ICLR 2019*.
- [16] Kristina Toutanova and Danqi Chen. 2015. Observed versus latent features for knowledge base and text inference. In *Proceedings of the 3rd Workshop on Continuous Vector Space Models and their Compositionality*. 57–66.

- [17] Théo Trouillon, Johannes Welbl, Sebastian Riedel, Éric Gaussier, and Guillaume Bouchard. 2016. Complex Embeddings for Simple Link Prediction. In *Proceedings of the 33th International Conference on Machine Learning*. 2071–2080.
- [18] A. Ungar. 2001. Hyperbolic trigonometry and its application in the Poincaré ball model of hyperbolic geometry. *Computers & Mathematics With Applications* 41 (2001), 135–147.
- [19] Quan Wang, Zhendong Mao, Bin Wang, and Li Guo. 2017. Knowledge Graph Embedding: A Survey of Approaches and Applications. *IEEE Transactions on Knowledge and Data Engineering* 29 (2017), 2724–2743.
- [20] Zhiwen Xie, Guangyou Zhou, Jin Liu, and Jimmy Xiangji Huang. 2020. ReInceptionE: Relation-Aware Inception Network with Joint Local-Global Structural Information for Knowledge Graph Embedding. In *Proceedings of the 58th Annual Meeting of the Association for Computational Linguistics, ACL 2020, Online, July 5-10, 2020*. 5929–5939.
- [21] Shuai Zhang, Yi Tay, Lina Yao, and Qi Liu. 2019. Quaternion Knowledge Graph Embeddings. In *Advances in Neural Information Processing Systems 32: Annual Conference on Neural Information Processing Systems 2019, NeurIPS 2019, December 8-14, 2019, Vancouver, BC, Canada*. 2731–2741.